Adaptive Fuzzy Finite-Time Command Filtered Impedance Control for Robotic Manipulators

GAORONG LIN, JINPENG YU, AND JIAPENG LIU
School of Automation, Qingdao University, Qingdao 266071, China
Shandong Key Laboratory of Industrial Control Technology, Qingdao University, Qingdao 266071, China

Corresponding author: Jinpeng Yu (yjp1109@hotmail.com)

ABSTRACT In order to improve the security and compliance of physical human-robot interaction (pHRI), an adaptive fuzzy impedance control for robotic manipulators based on finite-time command filtered method is proposed in this paper. Firstly, robots usually encounter system uncertainties in practical applications, and the adaptive fuzzy control is introduced to approximate the system uncertainties. Secondly, the finite-time control method is used to improve the interaction performance of the system. Then, the command filtered control technique is used to deal with the "computational complexity" of traditional backstepping. Finally, simulations are conducted to illustrate the effectiveness of the proposed control method in physical human-robot interaction.

INDEX TERMS Physical human-robot interaction (pHRI), adaptive fuzzy control, impedance control, finite-time control, command filtered control.

I. INTRODUCTION

In recent years, robots have been widely applied in social services, such as rehabilitation [1], home service [2], education and entertainment [3]. Physical human-robot interaction has become one of the active research fields in social service robots [4], [5]. It should be concerned that security and compliance should be guaranteed in pHRI. Hence, researchers pay more attention to how to design more effective control strategies to achieve better interaction effects. To regulate the physical interaction between humans and robots, impedance-based controllers have been widely used [6]–[8]. In addition, robots usually encounter system uncertainties in practical applications [9], [10], such as sensor error, and parameters change, which will affect the performance of the robot control if they are not handled properly. Therefore, it is crucial to study the effective impedance control approaches for robots, which ensure the physical interaction performance by dealing with robot system uncertainties.

During the past years, many research results show that fuzzy logic control plays a significant role in estimating the dynamic model of complex nonlinear systems [11], [12], and

The associate editor coordinating the review of this manuscript and approving it for publication was Choon Ki Ahn.

various impedance control approaches based on the adaptive control [13], [14] and fuzzy logic control [15]–[17] have been proposed for uncertain manipulators. Among these works, an impedance sliding mode control with adaptive fuzzy compensation scheme was proposed in [15] which employing adaptive fuzzy to estimate uncertain model. In [17], an adaptive fuzzy impedance control method where the fuzzy logic system (FLS) was used to approximate unknown nonlinear dynamics was exploited for pHRI. To improve interaction performance in pHRI, finite-time control [18]–[20] has been used in robotic manipulators. In [18], S. Yu introduced finite-time control into the robotic manipulator system, combined with terminal sliding mode technique to achieve a higher precision control performance and converge to the equilibrium in finite time. Up till now, the finite-time impedance control of uncertain manipulators has been seldom studied because it is extremely tough to eliminate the influence of manipulator uncertainty in the design of the finite-time impedance controller. Hence, it is a challenging work how to extend the finite-time impedance control to the uncertain manipulator to ensure the finite-time convergence of the control error.

In another research field, backstepping is one of the most effective control techniques for strict-feedback nonlinear systems, but the repeated derivatives of the virtual control

law in the backstepping control increase the "computational complexity " [21], [22]. For the sake of solving this problem, the dynamic surface control (DSC) was proposed by Swaroop *et al.* [23], Zhang and Ge [24], Yu *et al.* [25], but it doesn't take into account the problem of approximation errors generated by the first-order filters, and the control quality of the system may be affected. Therefore, Farrell *et al.* proposed command filtered control (CFC) [26]–[28], which solves approximation errors problem by some compensated signals, and reduces the complexity of the controller design. However, how to design the finite-time command filtered impedance control for the robotic manipulator systems is still a problem to be solved.

Based on the observations above, this paper proposes an adaptive fuzzy finite-time command filtered impedance control (AFFTCFIC) method for robotic manipulators to improve interaction performance. Adaptive fuzzy control is used to approximate the uncertain dynamics. The finite-time control was used to improve pHRI performance. CFC technique can deal with the issue of the "computational complexity " in the backstepping design, and overcome approximation errors problem for DSC by designing compensated signals. Lyapunov stability criterion is used for stability analysis. The primary contributions of the proposed control method can be summarized as follows:

- In the face of pHRI system, an AFFTCFIC scheme is proposed for the first time, which can achieve desired tracking performance in finite time. Hence, it expands the application scope for practical pHRI systems.
- Command filtered control technique with compensation signals is adopted to solve the problem of the "computational complexity " in the process of classical backstepping impedance controller design in [17].
- Compared with [15] and [17], the finite-time control can ensure the impedance control of the robot system with higher control accuracy and faster convergence speed. Therefore, it is introduced into the impedance control of the robotic manipulator, which can improve the interaction performance in pHRI system.

Notation: To facilitate the design of the AFFTCFIC. Let v_*^β be $v_*^\beta = \left[v_1^\beta, \ldots, v_i^\beta, \ldots, v_n^\beta \right]$, $(i = 1, \ldots, n.n \in N^*)$. The Euclidean norm of a vector is denoted by $\| * \|$. The maximum and minimum eigenvalues of the matrix $*$ are denoted by $\lambda_{\max} (*)$ and $\lambda_{\min} (*)$, respectively.

The rest of this study is arranged as follows. The mathematical model and preliminaries are given in Section *II*. AFFTCFIC controller design and stability analysis are presented in Sections *III* and *IV*. Simulink results and conclusions are shown in Sections *V* and *VI*.

II. MATHEMATICAL MODEL AND PRELIMINARIES
A. SYSTEM DESCRIPTION
Consider a physical human-robot interaction system, including a P-link manipulator and the force sensor mounted on the end-effector $(P \geq 1)$. A P-link manipulator dynamics [29] in

Cartesian space is described as

$$D (x) \ddot{x} + C (x, \dot{x}) \dot{x} + G (x) = \tau - \tau_e \qquad (1)$$

where $x, \dot{x}, \ddot{x} \in R^n$ are the position, velocity, acceleration vectors at the end-effector of the manipulator in Cartesian space, $D (x) \ddot{x} \in R^n$ denotes the inertia force vector of the manipulator in Cartesian space, $C (x, \dot{x}) \dot{x} \in R^n$ denotes the Centripetal and Coriolis force vector of the manipulator in Cartesian space, $G (x) \in R^n$ denotes the gravitational force vector of the manipulator in Cartesian space, $\tau \in R^n$ denotes the control input vector, $\tau_e \in R^n$ denotes the vector of constraining force on robotic end-effector in Cartesian space, which is 0 when the robotic manipulator is no contact with human or environment. n denotes the dimension of the operational space.

Property 1 ([30], [31]): The matrix $D (x)$ is symmetric positive definite.

Property 2 ([30], [31]): The matrix $\frac{1}{2} \dot{D} (x) - C (x, \dot{x})$ is skew-symmetric.

For the convenience, D, C and G represent $D (x)$, $C (x, \dot{x})$ and $G (x)$, respectively.

Let $x_1 = x$ and $x_2 = \dot{x}_1$. Equation (1) becomes

$$\dot{x}_2 = D^{-1} [\tau - \tau_e - Cx_2 - G] . \qquad (2)$$

When the manipulator comes into contact with human or environment, an interaction force will be generated based on the user-defined dynamics, the target impedance. The desired impedance dynamics in the workspace [32] is expressed as

$$M_d \ddot{e} + B_d \dot{e} + K_d e = \tau_e, \qquad (3)$$

where $e = x_d - x_r$, x_r denotes the commanded trajectory, x_d denotes the desired trajectory. the desired inertia, damping, and stiffness matrices are denoted by M_d, B_d, and K_d specified by the user, respectively. If the manipulator moves in free space, there has $x_r = x_d$ and $\tau_e = 0$. However, when the manipulator is in contact with the environment, the contact force of the end-effector is defined by the desired impedance dynamics (3). If x tracks x_r precisely, (3) becomes

$$M_d (\ddot{x}_d - \ddot{x}) + B_d (\dot{x}_d - \dot{x}) + K_d (x_d - x) = \tau_e.$$

It should be mentioned that τ_e can be measured from force sensor on robotic end-effector, M_d, B_d, K_d and x_d are defined by the user. Therefore, x_r can be calculated from (3).

B. FUZZY LOGIC SYSTEM
An FLS is composed of three parts: 1) the fuzzifier; 2) the fuzzy inference engine for processing fuzzy rules; and 3) the defuzzifier [33]–[35].

Consider l fuzzy IF-THEN rules $R^{(s)}$, $s = 1, \ldots, l$, where $R^{(s)}$ represents the sth rule. The fuzzifier maps the input point x_i in the input space $U \subset R^n$ to a fuzzy set A_i^s in the input space, and $x = [x_1, x_2, \ldots, x_n]^T \in U$ is the input vector of the fuzzy system. Membership functions of linguistic variable x_i for $i = 1, \ldots, n$ are used to represent fuzzy sets. The fuzzy inference engine implements a mapping from fuzzy sets in the

input space to fuzzy sets in the output space $V \subset R^m$ based on fuzzy rules, and $y = [y_1, y_2, \ldots, y_m]^T \in V$ is the output vector of the fuzzy system. Finally, the defuzzifier maps fuzzy sets in the output space V into a crisp output value. The fuzzy logic system is

$$y_j = \frac{\sum_{s=1}^{l} \left(\prod_{i=1}^{n} \mu_{A_i^s} \right) y_j^s}{\sum_{s=1}^{l} \left(\prod_{i=1}^{n} \mu_{A_i^s} \right)}, \quad j = 1, \ldots, m, \quad (4)$$

where $\mu_{A_i^s} = \exp \left[- \left(x_i - c_{is}^2 \right) / \sigma_{is}^2 \right]$. For the sake of clarity, the fuzzy basis function vector and weight vector are defined as $\phi(x, c, \sigma) = [p_1, p_2, \ldots, p_l]^T$ and $\theta_j = \left[y_j^1, y_j^2, \ldots, y_j^l \right]^T$, respectively, where $p_s = \left(\prod_{i=1}^{n} \mu_{A_i^s} \middle/ \sum_{s=1}^{l} \left(\prod_{i=1}^{n} \mu_{A_i^s} \right) \right)$, $\sigma = \left[\sigma_1^T, \sigma_2^T, \ldots, \sigma_n^T \right]^T$ and $c = \left[c_1^T, c_2^T, \ldots, c_n^T \right]^T$. Hence, (4) can be described as

$$y_j = \theta_j^T \phi(x, c, \sigma). \quad (5)$$

FLS can approximate any given continuous function $f_j(x)$, $j = 1, 2, \ldots, m$, to arbitrary accuracy on a compact set Ω. Hence, for any constant $\delta_j > 0$, there is a $\theta_j^{*T} \phi(x)$ in the FLS that makes

$$\sup_{x \in \Omega} \left| f_j(x) - \theta_j^{*T} \phi(x) \right| \leq \delta_j$$

where θ_j^* is an actual weight vector, ε_j is the approximation error, which on page satisfies $\max_{x \in \Omega} \|\varepsilon_j\| \leq \delta_j$.

C. PRELIMINARIES

Lemma 1 [36]: For any real numbers $\lambda_1 > 0$, $\lambda_2 > 0$, $0 < \beta < 1$, then the finite-time stable extension Lyapunov condition can be expressed as: $\dot{V}(x) \leq -\lambda_1 V(x) - \lambda_2 V^\beta(x)$, The convergence time by $T_r \leq t_0 + [1/\lambda_1(1 - \beta)] \ln \left[(\lambda_1 V^{1-\beta}(t_0) + \lambda_2)/\lambda_2 \right]$ to estimate.

Lemma 2 [37]: For $x_i \in R$, $i = 1, 2, \ldots, n$, $0 < p \leq 1$, then $\left(\sum_{i=1}^{n} |x_i| \right)^p \leq \sum_{i=1}^{n} |x_i|^p \leq n^{1-p} \left(\sum_{i=1}^{n} |x_i| \right)^p$.

Lemma 3 [38]: For real variables x and y, and given positive constants b_1, b_2, b_3, the following relation holds:

$$|x|^{b_1} |y|^{b_2} \leq \frac{b_2}{b_1 + b_2} b_3^{-\frac{b_1}{b_2}} |x|^{b_1 + b_2} + \frac{b_1}{b_1 + b_2} b_3 |y|^{b_1 + b_2}. \quad (6)$$

Lemma 4 ([39], [40]): The Levant differentiator is described as follows:

$$\begin{cases} \dot{\varphi}_1 = \iota_1 \\ \iota_1 = -R_1 \Delta \text{sign}(\varphi_1 - \alpha) + \varphi_2, \\ \dot{\varphi}_2 = -R_2 \text{sign}(\varphi_2 - \iota_1) \end{cases} \quad (7)$$

where $\Delta = \text{diag} \left(|\varphi_{11} - \alpha_{r1}|^{\frac{1}{2}}, \ldots, |\varphi_{1n} - \alpha_{rn}|^{\frac{1}{2}} \right)$. α is the input signal of the differentiator, $\varphi_1 = x_{1,c}$ and $\varphi_2 = \dot{x}_{1,c}$ are the output signals of the differentiator. Select properly parameters R_1 and R_2, the following equations are true when

there are no input noises after a transient process of the finite-time.

$$\varphi_1 = \alpha_0, \iota_1 = \dot{\alpha}_0,$$

and the differentiator's solutions have finite-time stability.

When the differentiator's input signal is given to be unaffected by noise, that is $\alpha = \alpha_0$. Consider the input noise satisfying the inequation $|\alpha - \alpha_0| \leq \kappa$. Thence, the following inequations completely dependent on differentiator parameters R_1 and R_2 hold in finite time:

$$\begin{cases} |\varphi_1 - \alpha_{r0}| \leq \vartheta_1 \kappa = \bar{\omega}_1 \\ |\iota_1 - \dot{\alpha}_{r0}| \leq \zeta_1 \kappa = \bar{\omega}_2, \end{cases}$$

where ϑ_1 and ζ_1 are normal numbers determined by the first-order Levant differentiator design parameters. $\bar{\omega}_1$ and $\bar{\omega}_2$ are normal numbers.

III. CONTROL DESIGN

According to the principle of backstepping method, the error variables are defined as follows:

$$z_1 = x_1 - x_r, z_2 = x_2 - x_{1,c}, \quad (8)$$

where $x_{1,c}$ is the first-order Levant differentiator's output signal when virtual control law α is the input signal. The error compensation signals are defined as $\xi_i = z_i - v_i$, $i = 1, 2$ with $\xi_i(0) = 0$. The specific structure of virtual control law and the error compensation signals are given in the following design.

Step1: Selecting a Lyapunov function as

$$V_1 = \frac{1}{2} v_1^T v_1. \quad (9)$$

Differentiating V_1 with respect to time yields

$$\dot{V}_1 = v_1^T \dot{v}_1 = v_1^T (\dot{z}_1 - \dot{\xi}_1) = v_1^T (x_2 - \dot{x}_r - \dot{\xi}_1). \quad (10)$$

Designing virtual control law α and compensation signal $\dot{\xi}_1$ as follows:

$$\alpha = -K_1 z_1 + \dot{x}_r - S_1 v_{1*}^\beta, \quad (11)$$

$$\dot{\xi}_1 = -K_1 \xi_1 + \xi_2 + (x_{1,c} - \alpha) - h_1 \text{sign}(\xi_1), \quad (12)$$

where the gain matrix $K_1 = K_1^T > 0$, $S_1 = S_1^T > 0$, the parameter $0 < \beta < 1$, $h_1 > 0$.

Substituting equations (11) and (12) into equation (10) yields

$$\dot{V}_1 = -v_1^T K_1 v_1 + v_1^T v_2 - v_1^T S_1 v_{1*}^\beta + h_1 v_1^T \text{sign}(\xi_1). \quad (13)$$

Step2: Then, selecting the Lyapunov function as

$$V_2 = V_1 + \frac{1}{2} v_2^T D v_2, \quad (14)$$

and taking its time derivative yields

$$\dot{V}_2 = \dot{V}_1 + v_2^T D \dot{v}_2 + \frac{1}{2} v_2^T \dot{D} v_2$$

$$= v_2^T \left(\begin{array}{c} \tau - \tau_e - G - C x_2 \\ + v_1 - D (\dot{x}_{1,c} + \dot{\xi}_2) \end{array} \right) - v_1^T K_1 v_1$$

$$- v_1^T S_1 v_{1*}^\beta + h_1 v_1^T \text{sign}(\xi_1) + \frac{1}{2} v_2^T \dot{D} v_2. \quad (15)$$

Since there are uncertainties in D, C and G, FLSs are used to approximate the uncertainties in D, C, and G. The fuzzy-approximation-based adaptive impedance control will be designed to approach the uncertain dynamics of the robotic manipulator and to adjust the interaction between human and manipulator.

Designing the control law τ as

$$\tau = -K_2 z_2 + \tau_e + \hat{\theta}_D^T \phi_D (Z_D) \dot{x}_{1,c} + \hat{\theta}_C^T \phi_C (Z_C) x_{1,c}$$
$$+ \hat{\theta}_G^T \phi_G (Z_G) - v_1 - S_2 v_{2*}^{\beta} - K_r \text{sign} (v_2), \quad (16)$$

where the gain matrix $K_2 = K_2^T > 0$, $S_2 = S_2^T > 0$, $K_r = \text{diag}[k_{rii}] > 0$. $\hat{\theta}_D$, $\hat{\theta}_C$ and $\hat{\theta}_G$ are the estimate weight matrices, θ_D^*, θ_C^* and θ_G^* are the actual weight matrices, $\tilde{\theta}_D = \hat{\theta}_D - \theta_D^*$, $\tilde{\theta}_C = \hat{\theta}_C - \theta_C^*$ and $\tilde{\theta}_G = \hat{\theta}_G - \theta_G^*$ are the weight error matrices, $Z_D = \left[x_1^T, x_2^T, x_{1,c}^T, \dot{x}_{1,c}^T \right]^T$, $Z_C = \left[x_1^T, x_2^T, x_{1,c}^T \right]^T$ and $Z_G = \left[x_1^T, x_2^T \right]^T$ are FLS inputs, respectively.

The updating laws are designed as

$$\dot{\hat{\theta}}_{Dk} = -\Gamma_{Dk} \left(\sigma_{Dk} \hat{\theta}_{Dk} + \phi_{Dk} (Z_D) \dot{x}_{1,c} v_{2k} \right), \quad (17)$$

$$\dot{\hat{\theta}}_{Ck} = -\Gamma_{Ck} \left(\sigma_{Ck} \hat{\theta}_{Ck} + \phi_{Ck} (Z_C) x_{1,c} v_{2k} \right), \quad (18)$$

$$\dot{\hat{\theta}}_{Gk} = -\Gamma_{Gk} \left(\sigma_{Gk} \hat{\theta}_{Gk} + \phi_{Gk} (Z_G) v_{2k} \right), \quad (19)$$

where $\Gamma_{Dk} > 0$, $\Gamma_{Ck} > 0$, $\Gamma_{Gk} > 0$, and σ_{Dk}, σ_{Ck}, σ_{Gk} are positive constants for improving the robustness. $\hat{\theta}_D^T \phi_D (Z_D)$ is an estimation matrix of $\theta_D^{*T} \phi_D (Z_D)$, $\hat{\theta}_C^T \phi_C (Z_C)$ is an estimation matrix of $\theta_C^{*T} \phi_C (Z_C)$ and $\hat{\theta}_G^T \phi_G (Z_G)$ is an estimation matrix of $\theta_G^{*T} \phi_G (Z_G)$.

$$\theta_D^{*T} \phi_D (Z_D) = D + \varepsilon_D, \quad (20)$$
$$\theta_C^{*T} \phi_C (Z_C) = C + \varepsilon_C, \quad (21)$$
$$\theta_G^{*T} \phi_G (Z_G) = G + \varepsilon_G, \quad (22)$$

where ε_D, ε_C, and ε_G are small approximation errors.

For the convenience of derivation, choosing $\dot{\xi}_2 = 0$. Substituting the control law (16) and equations (20)-(22) into (15) and Property 2 is used, there is

$$\dot{V}_2 = -v_1^T K_1 v_1 - v_1^T S_1 v_{1*}^{\beta} - v_2^T K_2 v_2 - v_2^T S_2 v_{2*}^{\beta}$$
$$+ v_2^T \tilde{\theta}_D^T \phi_D (Z_D) \dot{x}_{1,c} + v_2^T \tilde{\theta}_C^T \phi_C (Z_C) x_{1,c}$$
$$+ v_2^T \tilde{\theta}_G^T \phi_G (Z_G) + v_2^T (E_r - K_r \text{sign} (v_2))$$
$$+ h_1 v_1^T \text{sign} (\xi_1), \quad (23)$$

where $E_r = \varepsilon_D \dot{x}_{1,c} + \varepsilon_C x_{1,c} + \varepsilon_G$, E_{ri}, $i = 1, \ldots, n$ is ith element of a vector, there has $E_r = [E_{r1}, \ldots, E_{rn}]$.

IV. STABILITY ANALYSIS

For the stability analysis, the Lyapunov function is selected as

$$V = V_2 + \frac{1}{2} \sum_{k=1}^{n} \tilde{\theta}_{Dk}^T \Gamma_{Dk}^{-1} \tilde{\theta}_{Dk} + \frac{1}{2} \sum_{k=1}^{n} \tilde{\theta}_{Ck}^T \Gamma_{Ck}^{-1} \tilde{\theta}_{Ck}$$
$$+ \frac{1}{2} \sum_{k=1}^{n} \tilde{\theta}_{Gk}^T \Gamma_{Gk}^{-1} \tilde{\theta}_{Gk}. \quad (24)$$

Substituting (17)-(19) and (23) into the time derivative of (24) yields

$$\dot{V} = -v_1^T K_1 v_1 - v_1^T S_1 v_{1*}^{\beta} - v_2^T K_2 v_2 - v_2^T S_2 v_{2*}^{\beta}$$
$$+ v_2^T \tilde{\theta}_D^T \phi_D (Z_D) \dot{x}_{1,c} + v_2^T \tilde{\theta}_C^T \phi_C (Z_C) x_{1,c}$$
$$+ v_2^T \tilde{\theta}_G^T \phi_G (Z_G) + v_2^T (E_r - K_r \text{sign} (v_2))$$
$$- \sum_{k=1}^{n} \tilde{\theta}_{Dk}^T \phi_{Dk} (Z_D) \dot{x}_{1,c} v_{2k} - \sum_{k=1}^{n} \sigma_{Dk} \tilde{\theta}_{Dk}^T \hat{\theta}_{Dk}$$
$$- \sum_{k=1}^{n} \tilde{\theta}_{Ck}^T \phi_{Ck} (Z_C) x_{1,c} v_{2k} - \sum_{k=1}^{n} \sigma_{Ck} \tilde{\theta}_{Ck}^T \hat{\theta}_{Ck}$$
$$- \sum_{k=1}^{n} \tilde{\theta}_{Gk}^T \phi_{Gk} (Z_G) v_{2k} - \sum_{k=1}^{n} \sigma_{Gk} \tilde{\theta}_{Gk}^T \hat{\theta}_{Gk}$$
$$+ h_1 v_1^T \text{sign} (\xi_1), \quad (25)$$

nothing that

$$v_2^T \tilde{\theta}_D^T \phi_D (Z_D) \dot{x}_{1,c} = \sum_{k=1}^{n} \tilde{\theta}_{Dk}^T \phi_{Dk} (Z_D) \dot{x}_{1,c} v_{2k}, \quad (26)$$

$$v_2^T \tilde{\theta}_C^T \phi_C (Z_C) x_{1,c} = \sum_{k=1}^{n} \tilde{\theta}_{Ck}^T \phi_{Ck} (Z_C) x_{1,c} v_{2k}, \quad (27)$$

$$v_2^T \tilde{\theta}_G^T \phi_G (Z_G) = \sum_{k=1}^{n} \tilde{\theta}_{Gk}^T \phi_{Gk} (Z_G) v_{2k}. \quad (28)$$

Based on Young's inequality, there holds

$$-\tilde{\theta}_{Dk}^T \hat{\theta}_{Dk} \le -\frac{1}{2} \tilde{\theta}_{Dk}^T \tilde{\theta}_{Dk} + \frac{1}{2} \theta_{Dk}^{*T} \theta_{Dk}^*, \quad (29)$$

$$-\tilde{\theta}_{Ck}^T \hat{\theta}_{Ck} \le -\frac{1}{2} \tilde{\theta}_{Ck}^T \tilde{\theta}_{Ck} + \frac{1}{2} \theta_{Ck}^{*T} \theta_{Ck}^*, \quad (30)$$

$$-\tilde{\theta}_{Gk}^T \hat{\theta}_{Gk} \le -\frac{1}{2} \tilde{\theta}_{Gk}^T \tilde{\theta}_{Gk} + \frac{1}{2} \theta_{Gk}^{*T} \theta_{Gk}^*, \quad (31)$$

$$h_1 v_1^T \text{sign} (\xi_1) \le \frac{h_1}{2} v_1^T v_1 + \frac{nh_1}{2}. \quad (32)$$

Substituting (26)-(32) into (25) with $K_{rii} \ge \|E_{ri}\|$ yields

$$\dot{V} \le -v_1^T \left(K_1 - \frac{h_1}{2} \right) v_1 - v_1^T S_1 v_{1*}^{\beta} - v_2^T K_2 v_2$$
$$- v_2^T S_2 v_{2*}^{\beta} - \frac{1}{2} \sum_{k=1}^{n} \sigma_{Dk} \tilde{\theta}_{Dk}^T \tilde{\theta}_{Dk}$$
$$- \frac{1}{2} \sum_{k=1}^{n} \sigma_{Ck} \tilde{\theta}_{Ck}^T \tilde{\theta}_{Ck} - \frac{1}{2} \sum_{k=1}^{n} \sigma_{Gk} \tilde{\theta}_{Gk}^T \tilde{\theta}_{Gk}$$
$$+ \frac{1}{2} \sum_{k=1}^{n} \sigma_{Dk} \theta_{Dk}^{*T} \theta_{Dk}^* + \frac{1}{2} \sum_{k=1}^{n} \sigma_{Ck} \theta_{Ck}^{*T} \theta_{Ck}^*$$
$$+ \frac{1}{2} \sum_{k=1}^{n} \sigma_{Gk} \theta_{Gk}^{*T} \theta_{Gk}^* + \frac{nh_1}{2}. \quad (33)$$

Applying Lemma 3 to the terms $\left(\sum_{k=1}^{n} \frac{\sigma_{Dk} \tilde{\theta}_{Dk}^T \tilde{\theta}_{Dk}}{4} \right)^{\frac{\beta+1}{2}}$, $\left(\sum_{k=1}^{n} \frac{\sigma_{Ck} \tilde{\theta}_{Ck}^T \tilde{\theta}_{Ck}}{4} \right)^{\frac{\beta+1}{2}}$, $\left(\sum_{k=1}^{n} \frac{\sigma_{Gk} \tilde{\theta}_{Gk}^T \tilde{\theta}_{Gk}}{4} \right)^{\frac{\beta+1}{2}}$ with $y = 1$, and

$b_1 = \frac{\beta+1}{2}$, $b_2 = 1 - \frac{\beta+1}{2}$, $b_3 = \left(\frac{1-\beta}{2}\right)^{\frac{1-\beta}{1+\beta}}$, there holds

$$\left(\sum_{k=1}^{n} \frac{\sigma_{Dk}\tilde{\theta}_{Dk}^T\tilde{\theta}_{Dk}}{4}\right)^{\frac{\beta+1}{2}} \leq \frac{1}{4}\sum_{k=1}^{n}\sigma_{Dk}\tilde{\theta}_{Dk}^T\tilde{\theta}_{Dk} + b_1 b_3, \quad (34)$$

$$\left(\sum_{k=1}^{n} \frac{\sigma_{Ck}\tilde{\theta}_{Ck}^T\tilde{\theta}_{Ck}}{4}\right)^{\frac{\beta+1}{2}} \leq \frac{1}{4}\sum_{k=1}^{n}\sigma_{Ck}\tilde{\theta}_{Ck}^T\tilde{\theta}_{Ck} + b_1 b_3, \quad (35)$$

$$\left(\sum_{k=1}^{n} \frac{\sigma_{Gk}\tilde{\theta}_{Gk}^T\tilde{\theta}_{Gk}}{4}\right)^{\frac{\beta+1}{2}} \leq \frac{1}{4}\sum_{k=1}^{n}\sigma_{Gk}\tilde{\theta}_{Gk}^T\tilde{\theta}_{Gk} + b_1 b_3. \quad (36)$$

According to Lemma 2 and $v_j = [v_{j,1}, v_{j,2}, \ldots, v_{j,n}]^T$, there holds

$$v_j^T v_{j*}^{\beta} = [v_{j,1}, v_{j,2}, \ldots, v_{j,n}]\left[v_{j,1}^{\beta}, v_{j,2}^{\beta}, \ldots, v_{j,n}^{\beta}\right]^T$$
$$= v_{j,1}^{\beta+1} + v_{j,2}^{\beta+1} + \cdots + v_{j,n}^{\beta+1} \geq \left(v_j^T v_j\right)^{\frac{\beta+1}{2}}. \quad (37)$$

Substituting (34)-(37) into (33) yields

$$\dot{V} \leq -v_1^T\left(K_1 - \frac{h_1}{2}\right)v_1 - v_1^T S_1 v_{1*}^{\beta} - v_2^T K_2 v_2$$
$$-v_2^T S_2 v_{2*}^{\beta} - \frac{1}{4}\sum_{k=1}^{n}\sigma_{Dk}\tilde{\theta}_{Dk}^T\tilde{\theta}_{Dk}$$
$$-\frac{1}{4}\sum_{k=1}^{n}\sigma_{Ck}\tilde{\theta}_{Ck}^T\tilde{\theta}_{Ck} - \frac{1}{4}\sum_{k=1}^{n}\sigma_{Gk}\tilde{\theta}_{Gk}^T\tilde{\theta}_{Gk}$$
$$-\left(\sum_{k=1}^{n}\frac{\sigma_{Dk}\tilde{\theta}_{Dk}^T\tilde{\theta}_{Dk}}{4}\right)^{\frac{\beta+1}{2}} + \frac{1}{2}\sum_{k=1}^{n}\sigma_{Dk}\theta_{Dk}^{*T}\theta_{Dk}^*$$
$$-\left(\sum_{k=1}^{n}\frac{\sigma_{Ck}\tilde{\theta}_{Ck}^T\tilde{\theta}_{Ck}}{4}\right)^{\frac{\beta+1}{2}} + \frac{1}{2}\sum_{k=1}^{n}\sigma_{Ck}\theta_{Ck}^{*T}\theta_{Ck}^*$$
$$-\left(\sum_{k=1}^{n}\frac{\sigma_{Gk}\tilde{\theta}_{Gk}^T\tilde{\theta}_{Gk}}{4}\right)^{\frac{\beta+1}{2}} + \frac{1}{2}\sum_{k=1}^{n}\sigma_{Gk}\theta_{Gk}^{*T}\theta_{Gk}^*$$
$$+\frac{nh_1}{2} + 3b_1 b_3$$
$$\leq -aV - bV^{\frac{\beta+1}{2}} + c, \quad (38)$$

where $K_1 - \frac{h_1}{2} > 0$, $\frac{1}{2} \leq \frac{\beta+1}{2} \leq 1$,

$$a = \min\left\{\lambda_{\min}(2K_1 - h_1), \min_{k=1,\ldots,n}\frac{\sigma_{Dk}}{2\lambda_{\max}\left(\Gamma_{Dk}^{-1}\right)},\right.$$
$$\left.\frac{\lambda_{\min}(2K_2)}{\lambda_{\max}(D)}, \min_{k=1,\ldots,n}\left\{\frac{\sigma_{Ck}}{2\lambda_{\max}\left(\Gamma_{Ck}^{-1}\right)}, \frac{\sigma_{Gk}}{2\lambda_{max}\left(\Gamma_{Gk}^{-1}\right)}\right\}\right\}, \quad (39)$$

$$b = \min\left\{\begin{array}{l} \min_{k=1,\ldots,n}\left(\frac{\sigma_{Dk}}{2\lambda_{\max}\left(\Gamma_{Dk}^{-1}\right)}\right)^{\frac{\beta+1}{2}}, \lambda_{\min}(S_1)*\\[2ex] 2^{\frac{\beta+1}{2}}, \min_{k=1,\ldots,n}\left(\frac{\sigma_{Ck}}{2\lambda_{\max}\left(\Gamma_{Ck}^{-1}\right)}\right)^{\frac{\beta+1}{2}},\\[2ex] \min_{k=1,\ldots,n}\left(\frac{\sigma_{Gk}}{2\lambda_{\max}\left(\Gamma_{Gk}^{-1}\right)}\right)^{\frac{\beta+1}{2}}, \lambda_{\min}(S_2)*\\[2ex] \left(\frac{2}{\lambda_{\max}(D)}\right)^{\frac{\beta+1}{2}} \end{array}\right\}, \quad (40)$$

$$c = \frac{1}{2}\sum_{k=1}^{n}\sigma_{Dk}\theta_{Dk}^{*T}\theta_{Dk}^* + \frac{1}{2}\sum_{k=1}^{n}\sigma_{Ck}\theta_{Ck}^{*T}\theta_{Ck}^*$$
$$+\frac{1}{2}\sum_{k=1}^{n}\sigma_{Gk}\theta_{Gk}^{*T}\theta_{Gk}^* + 3b_1 b_3 + \frac{nh_1}{2}. \quad (41)$$

Rewrite (41) as follows

$$\dot{V} \leq -\left(a - \frac{c}{2V}\right)V - \left(b - \frac{c}{2V^{\frac{\beta+1}{2}}}\right)V^{\frac{\beta+1}{2}}. \quad (42)$$

From (42), selecting parameters can obtain $a > \frac{c}{2V}$, $b > \frac{c}{2V^{\frac{\beta+1}{2}}}$. By Lemma 1, $v_j(j = 1, 2)$ will be within the finite-time T_1 converge to the domain $\|v_j\| \leq \max\left\{\sqrt{c/a}, \sqrt{2(c/2b)^{\frac{2}{\beta+1}}}\right\}$.

Remark 1: Control parameters determine the radius of the tracking error domain, that is, the smaller radius of the tracking error domain can be ensured by the larger parameters $\lambda_{\max}(K_i)$ and $\lambda_{\max}(S_i)$.

Remark 2: In the control law, the K_r is chosen as $K_{rii} \geq \|E_{ri}\|$. For stability, K_r is chosen to be properly large. This is not very ideal due to the introduction of the chattering. Therefore, the control parameter K_r can be changed as $K_r = k_D\dot{x}_{1,c} + k_C x_{1,c} + k_G$, where $k_D \geq \|\varepsilon_D\|$, $k_C \geq \|\varepsilon_C\|$, $k_G \geq \|\varepsilon_G\|$.

Theorem 1: Consider manipulator dynamics (1) with Property 1, 2 and impedance dynamics (3). If the finite-time command filter and the error compensation mechanism are chosen as (7), (12), and the adaptive FLS control law (16) with updating laws (17)-(19) are chosen, the tracking error z_1 converges to a small enough region with the radius $\max\left\{\sqrt{c/a}, \sqrt{2(c/2b)^{\frac{2}{\beta+1}}}\right\} + \max\left\{\sqrt{c_0/a_0}, \sqrt{2(c_0/2b_0)^2}\right\}$ in finite time $T \geq \max\{T_1, T_2\}$.

The proof of Theorem 1 is given in the Appendix.

Remark 3: In the proof of Theorem 1, the result $|x_{1,c} - \alpha| \leq \bar{w}_1$ from Lemma 4 will be used. Note that if the α of the finte-time command filter (7) is not influenced by the noise, there has $\bar{w}_1 = 0$. Therefore, the conclusion of Theorem 1 can be obtained when the noise is bounded.

Remark 4: Note that the manipulator is a highly nonlinear system. The finite-time convergence speed in the nonlinear
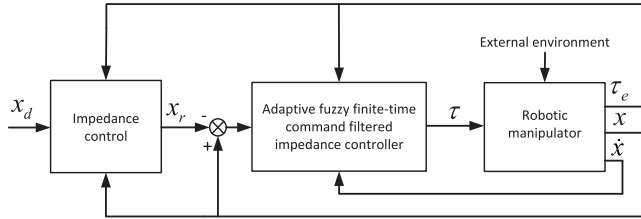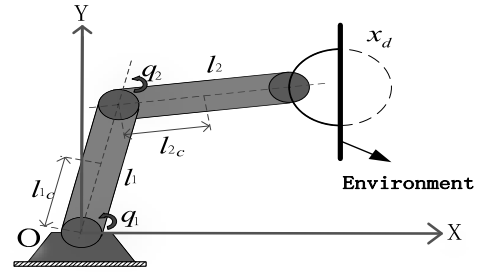
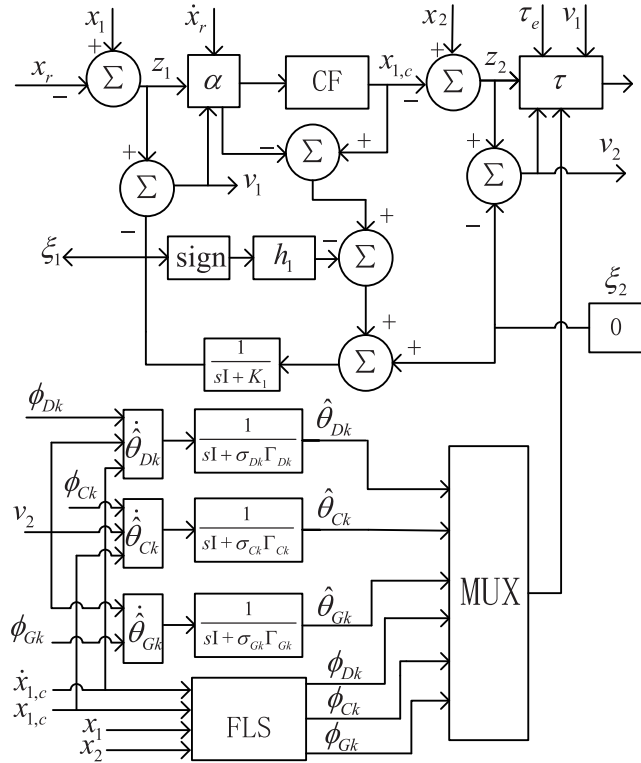**FIGURE 1.** Block diagram of control system.

FIGURE 2. Block diagram of the proposed method for manipulators.

FIGURE 3. A planar 2-DOF manipulator.

two rotary degrees of freedom is defined by (2), it can be described as follows:

$$\begin{cases} \dot{x}_1 = x_2 \\ \dot{x}_2 = D^{-1}\left[\tau - \tau_e - Cx_2 - G\right], \\ y = x_1 \end{cases}$$

and $x_1 = [x_{11}, x_{12}]^T$ and $x_2 = [\dot{x}_{11}, \dot{x}_{12}]^T$, x_{11} and x_{12} represent respectively the position of the axis X and Y on the end-effector of the manipulator in the Cartesian coordinates. $fe = \|\tau_e\|$ denotes the external force on the end-effector. $q = [q_1, q_2]^T$ represents the each joint angle position. m_i and l_i are respectively the mass and length of link i, l_{ci} is the distance from joint $i-1$ of the robotic manipulator to the centroid of the link i, I_i is the moment of inertia of link i through the centroid of link i, $(i = 1, 2)$ based on the axis of the page.

The inertia matrix of 2-DOF manipulator D_*, Centripetal and Coriolis matrix C_*, gravity force vector G_* are given as follows:

$$D_* = \begin{bmatrix} m_1 l_{c1}^2 + m_2 l_1^2 + l_{c2}^2 + 2l_1 l_{c2}\cos q_2 + I_1 + I_2 \\ m_2\left(l_{c2}^2 + l_1 l_{c2}\cos q_2\right) + I_2 \\ m_2\left(l_{c2}^2 + l_1 l_{c2}\cos q_2\right) + I_2 \\ m_2 l_{c2}^2 + I_2 \end{bmatrix}$$

$$C_* = \begin{bmatrix} -m_2 l_1 l_{c2}\dot{q}_2 \sin q_2 & -m_2 l_1 l_{c2}\left(\dot{q}_1 + \dot{q}_2\right)\sin q_2 \\ m_2 l_1 l_{c2}\dot{q}_1 \sin q_2 & 0 \end{bmatrix}$$
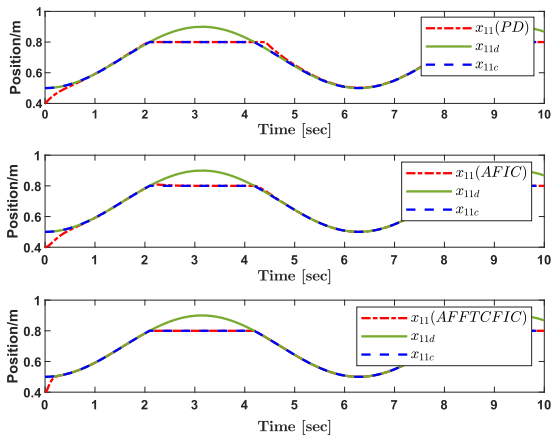
$$G_* = \begin{bmatrix} (m_1 l_{c2} + m_2 l_1)\, g\cos q_1 + m_2 l_{c2} g\cos(q_1 + q_2) \\ m_2 l_{c2} g\cos(q_1 + q_2) \end{bmatrix}$$

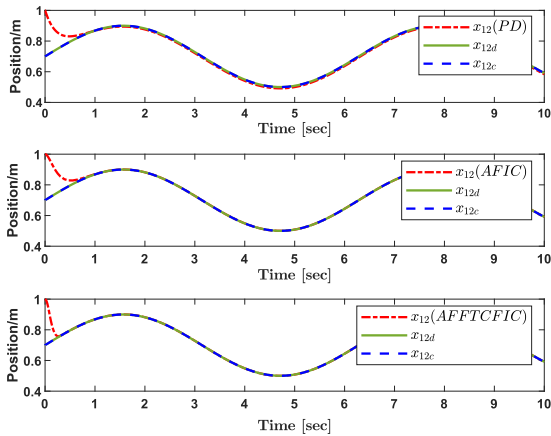The Jacobian matrix of 2-DOF robotic manipulator is shown as follows:

$$J = \begin{bmatrix} -(l_1 \sin q_1 + l_2 \sin(q_1 + q_2)) & -l_2 \sin(q_1 + q_2) \\ l_1 \cos q_1 + l_2 \cos(q_1 + q_2) & l_2 \cos(q_1 + q_2) \end{bmatrix}$$

Some formulas for robotic system are $D = J^{-T}D_* J^{-1}$, $C = J^{-T}\left(C_* - D_* J^{-1}\dot{J}\right)J^{-1}$ and $G = J^{-T}G_*$.

The parameters of the 2-DOF manipulator are shown as the length of link 1 and link 2 are 1.00m, the mass of link 1 and link 2 are 1.00kg, the moment of inertia of link 1 and link 2 are 0.25kg·m². The initial parameters of the robotic manipulator are $x_{11}(0) = 0.4, x_{12}(0) = 1$m, $\dot{x}_{11}(0) = \dot{x}_{12}(0) = 0$, $q_1(0) = \frac{\pi}{2}$, $q_2(0) = -\frac{\pi}{2}$, the desired trajectory of the 2-DOF robotic manipulator is shown as

system cannot be guaranteed by the traditional PID control. When the nonlinear system contains unknown dynamics, the excellent tracking performance cannot be guaranteed by the PID control. Although the excellent robustness and fast convergence capability of the unknown manipulator system can be guaranteed by the sliding mode control, the sliding mode control can only deal with the matched unknown dynamics, and the control effect cannot be ensured when the nonlinear system contains the unmatched unknown dynamics. When the robot system contains an unmatched unknown dynamics, the AFFTCFIC can ensure that the control error variable z_1 converges to a small enough domain of the origin in finite time, and that all signals in the robot system can be kept in the appropriate region in finite time.

V. SIMULATION RESULT
In this section, a 2-degrees of freedom (2-DOF) robotic manipulator on a vertical plane, which is shown in Fig.3, is considered, simulations of pHRIs verify the validity of the proposed method and the robotic manipulator system of

(a) The tracking curves on X-axis

(a) The tracking curves on Y-axis

FIGURE 4. The tracking curves under three schemes.

FIGURE 5. The tracking error curves under three schemes.
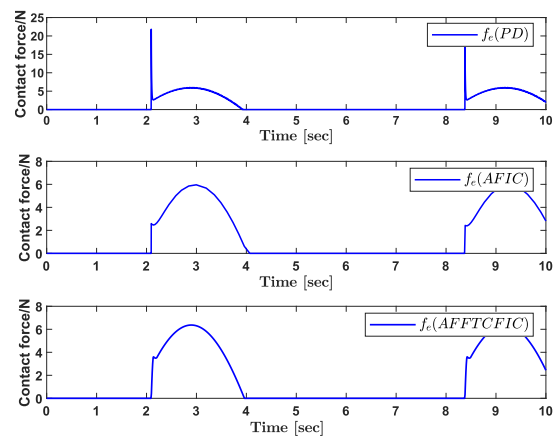
FIGURE 6. The external force curves under three schemes.
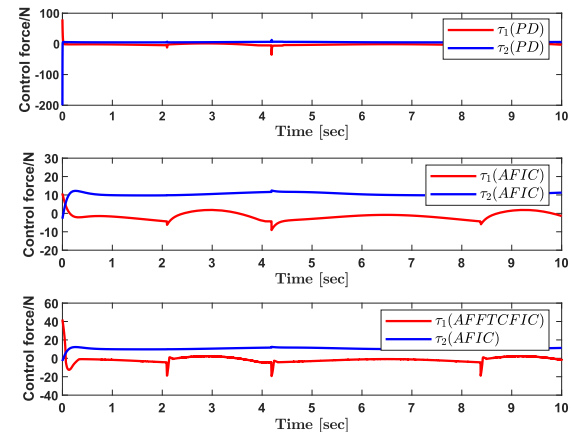
FIGURE 7. The control input curves under three schemes.

$x_d = [0.7 - 0.2\cos(t), 0.7 + 0.2\sin(t)]^T$, where $t \in [0, 10]$. The manipulator end-effector moves along the solid wall when it makes touch with the wall, and the obstacle wall is located as $x_o = 0.8$m.

The target impedance of the 2-DOF robotic manipulator is selected as $M_d = \text{diag}[1.0, 1.0]$, $B_d = \text{diag}[15.0, 15.0]$, $K_d = \text{diag}[60.0, 60.0]$.

The updating law parameters are $\Gamma_{Dk} = \Gamma_{Ck} = \Gamma_{Gk} = \text{diag}[20, 20]$, $\sigma_{Dk} = \sigma_{Dk} = \sigma_{Dk} = \text{diag}[0.01, 0.01]$.

In this part, the PD control method, the adaptive fuzzy impedance control (AFIC) method in [17] and the proposed AFFTCFIC method in this paper are compared. The robotic manipulator system control parameters are chosen as follows:

A). For PD method of the 2-DOF robotic manipulator, the control law is given as $\tau = -K_1 z_1 - K_2 z_2$ and control parameters are chosen as $K_1 = \text{diag}[800, 800]$, $K_2 = \text{diag}[200, 200]$;

B). For AFIC method of the 2-DOF robotic manipulator in [17], control parameters are given as $K_1 = \text{diag}[6, 6]$, $K_2 = \text{diag}[8, 8]$;

C). For AFFTCFIC method of the 2-DOF robotic manipulator, control the control parameters are given as $K_1 = \text{diag}[6, 6]$, $K_2 = \text{diag}[8, 8]$, $S_1 = \text{diag}[2, 2]$, $S_2 = \text{diag}[2, 2]$, $\gamma = 0.6$, $h_1 = 1$, $R_1 = 20$, $R_2 = 0.6$.

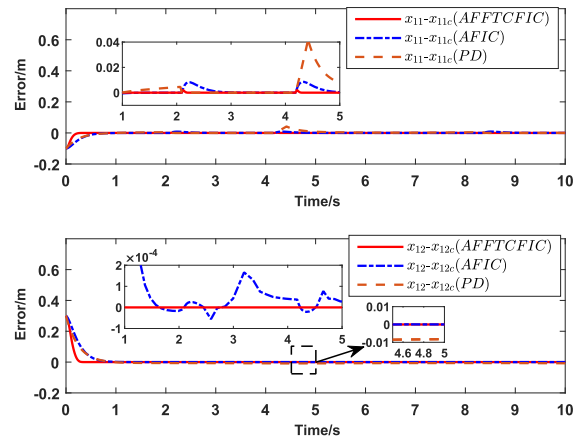The simulation results are described in Figs.4-8. Among them, Fig.4(a) and Fig.4(b) show the position tracking curves of the manipulator end-effector on the X-axis and Y-axis under three schemes. Fig.5 shows the position tracking error curves of the manipulator end-effector on the X-axis and Y-axis under three schemes. Indicated from Fig.4 to Fig.5, it can be seen that the tracking performances are better under the proposed control method whether the manipulator contact with the wall or not, and the proposed AFFTCFIC scheme
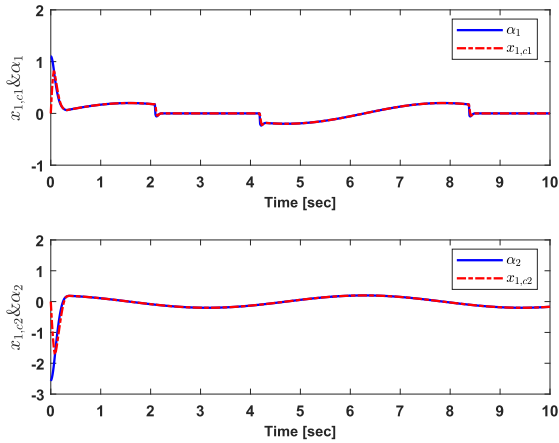
FIGURE 8. The curves of α and $x_{1,c}$ under the proposed algorithm.

has better control accuracy and faster convergence speed than the AFIC algorithm in [17] and PD algorithm. Figs.6 shows contact forces from the wall on X-axis. When the manipulator contacts with the solid wall, it can be seen that the desired impedance model can be obtained more smoothly and quickly under the AFFTCFIC method and PD control has a relatively large collision force in Fig.6. Fig.7 shows the control inputs are in proper bounds, but the PD control input is relatively large, which is not conducive to practical application. Fig.8 shows that the filtered signal $x_{1,c}$ has an excellent tracking approximation to the virtual signal α.

VI. CONCLUSION

In this paper, the adaptive fuzzy impedance controller that combines the finite-time control and the CFC technique has been proposed to improve the security and compliance of pHRI. The manipulator tracking quality has been improved by the finite-time control technique. Simultaneously, the combination of the CFC technique and the backstepping can solve the "computational complexity" issue in the backstepping controller design. Through the Lyapunov stability analysis and simulations, the validity of the proposed method is proven. Our future research is to design a novel finite-time state constraint control scheme of robotic manipulators, which can ensure that the manipulator moves in a finite space and achieves the desired performance in finite time.

APPENDIX
Proof of the Theorem 1

Proof: Now the following Lyapunov function is selected.

$$\bar{V} = \frac{1}{2}\xi_1^T \xi_1. \tag{43}$$

The differential of (43), with respect to time, is

$$\dot{\bar{V}} = -\xi_1^T K_1 \xi_1 + \xi_1^T \left(x_{1,c} - \alpha\right) - h_1 \xi_1^T \operatorname{sign}\left(\xi_1\right). \tag{44}$$

Based on Lemma 2 and Young's inequality, there holds

$$h_1 \xi_1^T \operatorname{sign}\left(\xi_1\right) \geq h_1 \left(\xi_1^T \xi_1\right)^{\frac{1}{2}}, \tag{45}$$

let $d = \left(x_{1,c} - \alpha\right)$, there holds

$$\xi_1^T d \leq \frac{1}{2}\xi_1^T \xi_1 + \frac{1}{2}d^T d. \tag{46}$$

According to Lemma 4, there is $\left|x_{1,c} - \alpha\right| \leq \bar{w}_1$ in finite time T_2, and substituting (45) and (46) into (44). For $t > T_2$, there holds

$$\dot{\bar{V}} \leq -\xi_1^T \left(K_1 - \frac{1}{2}I\right)\xi_1 - h_1\left(\xi_1^T \xi_1\right)^{\frac{1}{2}} + \frac{1}{2}\bar{w}_1^2$$
$$\leq -a_0 \bar{V} - b_0 \bar{V}^{\frac{1}{2}} + c_0, \tag{47}$$

where $K_1 - \frac{1}{2}I > 0$,

$$a_0 = 2 * \lambda_{\min}\left(K_1 - \frac{1}{2}I\right), b_0 = h_1 * 2^2, c_0 = \frac{1}{2}\bar{w}_1^2.$$

Rewrite (47) as follows

$$\dot{\bar{V}} \leq -\left(a_0 - \frac{c_0}{2\bar{V}}\right)\bar{V} - \left(b_0 - \frac{c_0}{2\bar{V}^{\frac{1}{2}}}\right)\bar{V}^{\frac{1}{2}}. \tag{48}$$

From (48), selecting parameters can obtain $a_0 - \frac{c_0}{2\bar{V}} > 0$, $b_0 - \frac{c_0}{2\bar{V}^{\frac{1}{2}}} > 0$. By Lemma 1, ξ_1 can converge to the domain $\|\xi_1\| \leq \max\left\{\sqrt{c_0/a_0}, \sqrt{2\left(c_0/2b_0\right)^2}\right\}$ in finite-time T_2. Since $z_1 = v_1 + \xi_1$, when $T \geq \max\{T_1, T_2\}$, there can obtain $\|z_1\| \leq \|v_1\| + \|\xi_1\| \leq \max\left\{\sqrt{c/a}, \sqrt{2\left(c/2b\right)^{\frac{2}{\beta+1}}}\right\} + \max\left\{\sqrt{c_0/a_0}, \sqrt{2\left(c_0/2b_0\right)^2}\right\}$. The proof is completed. ∎

REFERENCES

[1] W. He, S. S. Ge, Y. Li, E. Chew, and Y. S. Ng, "Neural network control of a rehabilitation robot by state and output feedback," *J. Intell. Robot. Syst.*, vol. 80, no. 1, pp. 15–31, Oct. 2015.

[2] Z. Kuang, Y. Yang, T. Hau, and Y. He, "Research on biomimetic coordination action of service robot based on stereo vision," in *Proc. 2nd IEEE Adv. Inf. Manage., Communicates, Electron. Autom. Control Conf. (IMCEC)*, May 2018, pp. 769–773.

[3] A. Ming, K. Enomoto, M. Shinozaki, R. Sato, and M. Shimojo, "Development of an entertainment robot system using Kinect," in *Proc. 10th France-Jpn./ 8th Eur.-Asia Congr. Mecatronics (MECATRONICS-Tokyo)*, Nov. 2014, pp. 127–132.

[4] R. Parasuraman, T. B. Sheridan, and C. D. Wickens, "A model for types and levels of human interaction with automation," *IEEE Trans. Syst., Man, Cybern. A, Syst. Humans*, vol. 30, no. 3, pp. 286–297, May 2000.

[5] M. Thabet, M. Patacchiola, and A. Cangelosi, "Sample-efficient deep reinforcement learning with imaginary rollouts for human-robot interaction," in *Proc. IEEE/RSJ Int. Conf. Intell. Robots Syst. (IROS)*, Nov. 2019, pp. 5079–5085.

[6] N. Hogan, "Impedance control of industrial robots," *Robot. Comput.-Integr. Manuf.*, vol. 1, no. 1, pp. 97–113, Jan. 1984.

[7] R. J. Anderson and M. W. Spong, "Hybrid impedance control of robotic manipulators," *IEEE J. Robot. Autom.*, vol. 4, no. 5, pp. 549–556, Oct. 1988.

[8] C.-C. Cheah and D. Wang, "Learning impedance control for robotic manipulators," *IEEE Trans. Robot. Autom.*, vol. 14, no. 3, pp. 452–465, Jun. 1998.

[9] Y. Pan, X. Li, and H. Yu, "Efficient PID tracking control of robotic manipulators driven by compliant actuators," *IEEE Trans. Control Syst. Technol.*, vol. 27, no. 2, pp. 915–922, Mar. 2019.

[10] J. A. Meda-Campana, "On the estimation and control of nonlinear systems with parametric uncertainties and noisy outputs," *IEEE Access*, vol. 6, pp. 31968–31973, 2018.

[11] Z. Li, C.-Y. Su, G. Li, and H. Su, "Fuzzy approximation-based adaptive backstepping control of an exoskeleton for human upper limbs," *IEEE Trans. Fuzzy Syst.*, vol. 23, no. 3, pp. 555–566, Jun. 2015.

[12] S. Hussain, K. B. Lee, M. A. Ahmed, B. Hayes, and Y. C. Kim, "Two-stage fuzzy logic inference algorithm for maximizing the quality of performance under the operational constraints of power grid in electric vehicle parking lots," *Energies*, vol. 13, no. 18, pp. 1–31, 2020.

[13] J.-J.-E. Slotine and W. Li, "Composite adaptive control of robot manipulators," *Automatica*, vol. 25, no. 4, pp. 509–519, Jul. 1989.

[14] M. Sharifi and H. Sayyaadi, "Nonlinear robust adaptive Cartesian impedance control of UAVs equipped with a robot manipulator," *Adv. Robot.*, vol. 29, no. 3, pp. 171–186, Feb. 2015.

[15] L. Kong, W. He, C. Yang, Z. Li, and C. Sun, "Adaptive fuzzy control for coordinated multiple robots with constraint using impedance learning," *IEEE Trans. Cybern.*, vol. 49, no. 8, pp. 3052–3063, Aug. 2019.

[16] H. Hu, X. Wang, and L. Chen, "Impedance sliding mode control with adaptive fuzzy compensation for robot-environment interacting," *IEEE Trans. Cybern.*, vol. 49, no. 8, pp. 3052–3063, 2019.

[17] P. Li, S. S. Ge, and C. Wang, "Impedance control for human-robot interaction with an adaptive fuzzy approach," in *Proc. 29th Chin. Control Decis. Conf. (CCDC)*, May 2017, pp. 5889–5894.

[18] S. Yu, X. Yu, B. Shirinzadeh, and Z. Man, "Continuous finite-time control for robotic manipulators with terminal sliding mode," *Automatica*, vol. 41, no. 11, pp. 1957–1964, Nov. 2005.

[19] L. Zhao, J. Yu, and Q.-G. Wang, "Adaptive finite-time containment control of uncertain multiple manipulator systems," *IEEE Trans. Cybern.*, early access, Apr. 6, 2020, doi: 10.1109/TCYB.2020.2981090.

[20] M. Van, S. S. Ge, and H. Ren, "Finite time fault tolerant control for robot manipulators using time delay estimation and continuous nonsingular fast terminal sliding mode control," *IEEE Trans. Cybern.*, vol. 47, no. 7, pp. 1681–1693, Jul. 2017.

[21] J. Yu, P. Shi, J. Liu, and C. Lin, "Neuroadaptive finite-time control for nonlinear MIMO systems with input constraint," *IEEE Trans. Cybern.*, early access, Nov. 17, 2020, doi: 10.1109/TCYB.2020.3032530.

[22] S. Ling, H. Wang, and P. X. Liu, "Adaptive fuzzy tracking control of flexible-joint robots based on command filtering," *IEEE Trans. Ind. Electron.*, vol. 67, no. 5, pp. 4046–4055, May 2020, doi: 10.1109/tie.2019.2920599.

[23] D. Swaroop, J. K. Hedrick, P. P. Yip, and J. C. Gerdes, "Dynamic surface control for a class of nonlinear systems," *IEEE Trans. Autom. Control*, vol. 45, no. 10, pp. 1893–1899, Oct. 2000.

[24] T. P. Zhang and S. S. Ge, "Adaptive dynamic surface control of nonlinear systems with unknown dead zone in pure feedback form," *Automatica*, vol. 44, no. 7, pp. 1895–1903, Jul. 2008.

[25] J. Yu, P. Shi, W. Dong, B. Chen, and C. Lin, "Neural network-based adaptive dynamic surface control for permanent magnet synchronous motors," *IEEE Trans. Neural Netw. Learn. Syst.*, vol. 26, no. 3, pp. 640–645, Mar. 2015.

[26] J. A. Farrell, M. Polycarpou, M. Sharma, and W. Dong, "Command filtered backstepping," *IEEE Trans. Autom. Control*, vol. 54, no. 6, pp. 1391–1395, Jun. 2009.

[27] W. Dong, J. A. Farrell, M. M. Polycarpou, V. Djapic, and M. Sharma, "Command filtered adaptive backstepping," *IEEE Trans. Control Syst. Technol.*, vol. 20, no. 3, pp. 566–580, May 2012.

[28] J. Yu, P. Shi, X. Chen, and G. Cui, "Finite-time command filtered adaptive control for nonlinear systems via immersion and invariance," *Sci. China Inf. Sci.*, 2020. [Online]. Available: https://engine.scichina.com/doi/10.1007/s11432-020-3144-6, doi: 10.1007/s11432-020-3144-6.

[29] S. S. Ge, T. H. Lee, and C. J. Harris, *Adaptive Neural Network Control of Robotic Manipulators*. London, U.K.: World Science, 1998.

[30] W. He, Y. Chen, and Z. Yin, "Adaptive neural network control of an uncertain robot with full-state constraints," *IEEE Trans. Cybern.*, vol. 46, no. 3, pp. 620–629, Mar. 2016.

[31] T. Sun, L. Peng, L. Cheng, Z.-G. Hou, and Y. Pan, "Composite learning enhanced robot impedance control," *IEEE Trans. Neural Netw. Learn. Syst.*, vol. 31, no. 3, pp. 1052–1059, Mar. 2020.

[32] M. Sharifi, S. Behzadipour, and G. R. Vossoughi, "Model reference adaptive impedance control in Cartesian coordinates for physical human–robot interaction," *Adv. Robot.*, vol. 28, no. 19, pp. 1277–1290, Oct. 2014.

[33] L.-X. Wang, "Design and analysis of fuzzy identifiers of nonlinear dynamic systems," *IEEE Trans. Autom. Control*, vol. 40, no. 1, pp. 11–23, Jan. 1995.

[34] F. C. Sun, Z. Q. Sun, and G. Feng, "An adaptive fuzzy controller based on sliding mode for robot manipulators," *IEEE Trans. Syst., Man, Cybern. B. Cybern.*, vol. 29, no. 5, pp. 661–667, Oct. 1999.

[35] S. Hussain, M. A. Ahmed, and Y.-C. Kim, "Efficient power management algorithm based on fuzzy logic inference for electric vehicles parking lot," *IEEE Access*, vol. 7, pp. 65467–65485, 2019.

[36] G. Cui, J. Yu, and P. Shi, "Observer-based finite-time adaptive fuzzy control with prescribed performance for nonstrict-feedback nonlinear systems," *IEEE Trans. Fuzzy Syst.*, early access, Dec. 31, 2021, doi: 10.1109/TFUZZ.2020.3048518.

[37] X. Huang, W. Lin, and B. Yang, "Global finite-time stabilization of a class of uncertain nonlinear systems," *Automatica*, vol. 41, no. 5, pp. 881–888, May 2005.

[38] F. Wang, B. Chen, X. Liu, and C. Lin, "Finite-time adaptive fuzzy tracking control design for nonlinear systems," *IEEE Trans. Fuzzy Syst.*, vol. 26, no. 3, pp. 1207–1216, Jun. 2018.

[39] A. Levant, "Higher-order sliding modes, differentiation and output-feedback control," *Int. J. Control*, vol. 76, nos. 9–10, pp. 924–941, Jan. 2003.

[40] C. Fu, Q.-G. Wang, J. Yu, and C. Lin, "Neural network-based finite-time command filtering control for switched nonlinear systems with backlash-like hysteresis," *IEEE Trans. Neural Netw. Learn. Syst.*, early access, Jul. 31, 2020, doi: 10.1109/TNNLS.2020.3009871.

GAORONG LIN received the B.Sc. degree in electrical engineering and automation from Fujian Agriculture and Forestry University, Fuzhou, China, in 2017. He is currently pursuing the M.Sc. degree in control science and engineering with Qingdao University, Qingdao, China.

His research interests include robotics and intelligent control.

JINPENG YU received the B.Sc. degree in automation from Qingdao University, Qingdao, China, in 2002, the M.Sc. degree in system engineering from Shandong University, Jinan, China, in 2006, and the Ph.D. degree from the Institute of Complexity Science, Qingdao University, in 2011. He is currently a Distinguished Professor with the School of Automation, Qingdao University. His research interests include electrical energy conversion and motor control, applied nonlinear control, and intelligent systems. He was a recipient of the Shandong Province Taishan Scholar Special Project Fund and the Shandong Province Fund for Outstanding Young Scholars.

JIAPENG LIU received the M.Sc. degree in control science and engineering from Qingdao University, Qingdao, China, in 2015, and the Ph.D. degree in engineering from Shandong University, Jinan, China, in 2019. He is currently a Distinguished Professor with the School of Automation, Qingdao University. His research interests include electrical energy conversion, ejector refrigeration, and model predictive control.